ANL-6463

ANL-6463

Argonne National Laboratory

EFFECTS OF SPIN-ORBIT COUPLING IN Si AND Ge

by

L. Liu

ANL-6463
Physics
(TID-4500, 16th Ed., Amended)
AEC Research and Development Report

ARGONNE NATIONAL LABORATORY
9700 South Cass Avenue
Argonne, Illinois

EFFECTS OF SPIN-ORBIT COUPLING IN Si AND Ge

by

L. Liu

Submitted in Partial Fulfillment of the
Requirements of the Degree of
Doctor of Philosophy in Physics
at The University of Chicago

November 1961

Operated by The University of Chicago
under
Contract W-31-109-eng-38

ABSTRACT

A treatment of spin-orbit effects in some semiconductors is given using the effective mass method and orthogonalized-plane-wave type wave functions. In this formalism, the spin-orbit splitting of valence states in the crystal is expressed directly in terms of either experimental or calculated values of the spin-orbit splitting of the atomic core states. The calculation yields values in good agreement with experiments for the splitting at $\Gamma_{25'}$ for Si and at both $\Gamma_{25'}$ and $L_{3'}$ for Ge. A demonstration is given of the enhancement of the spin-orbit splitting of valence states in the crystal over the corresponding atomic value.

The shift in the g-tensor due to spin-orbit interactions is studied in Si and Ge. Because of crystal selection rules, the usual two band approximation to the effective mass sum rule is inadequate for Si and, in particular, the core state must be considered. When all important states are included, the calculations yield values in good agreement with

experiment. In the case of Ge, it is found that core states do not contribute appreciably to the g-tensor. However, the calculated value for the shift in the transverse component of the g-tensor has an opposite sign to the measured one.

A certain matrix element of the deformation potential for Si is also evaluated based on the measured shift in the g-value due to strain. The result is compared with other deformation potentials in Si.

TABLE OF CONTENTS

I. INTRODUCTION

The effects of spin-orbit (s-o) coupling on the electronic properties of crystals have been discussed by several authors.[1-6] For semiconductors, these properties are largely determined by the nature of the conduction and valence band edges. In semiconductors where these band edges are of p atomic symmetry and split under the s-o interaction, knowledge of the magnitude of their s-o splittings becomes necessary in any quantitative calculations. Although there have been recently several direct measurements of the valence state s-o splitting for Si[7] and Ge[8] by optical experiments, there is lack of any quantitative estimate in theory. In this work we attempt to estimate the s-o splitting of valence states in crystals by treating the s-o interaction as a perturbation on the crystal states described by orthogonalized-plane-wave (OPW) type wave functions, which are well suited to most semiconductors. But prior to this calculation, we treat the s-o splitting of the atomic valence wave function, which, just like an OPW crystal wave function, consists of a smooth part plus

occupied core orbitals. In this way, we can make a comparison between the splitting in the atom and that in the crystal and then demonstrate why the splitting gets enhanced in the crystal. Since both the atomic valence wave function we use and the OPW crystal wave function contain core orbitals, the s-o splitting of valence states in the atom and in the crystal can be expressed in terms of the s-o splitting of the atomic core states in our formalism. We apply the splitting calculations to crystalline Si and Ge and obtain values in good agreement with experiment.

The effect of s-o interaction on the magnetic resonance is first of all a shift in the isotropic g-value for conduction (or valence) electrons from the free electron value of 2.0023. Furthermore, when for some semiconductors like Si and Ge the conduction band edge consists of several valleys lying in equivalent positions along certain symmetry directions in the Brillouin zone (B.Z.), the s-o interaction introduces an anisotropy into the single valley g-value, which can be expressed as a tensorial quantity. Theoretical treatment of the g-tensor for semiconductors or semimetals has been done in the framework of the effective mass approximation. In the absence of crystal wave functions, a two level approximation to the effective mass sum rule was further assumed to evaluate

the g-tensor for certain materials.[3-5] In other words, for semiconductors, it was assumed that the major contribution to the g-shift for conduction (valence) electrons came from the s-o splitting of the nearest valence (conduction) level. Roth in this way has obtained excellent quantitative agreement with experiment for the longitudinal g-shift in Ge[4] and the isotropic g-value for InSb.[3] However, the two level approximation is not always adequate. A typical semiconductor which illustrates this failure is Si. The Si valence s-o splitting at the conduction edge is very small due to special selection rules, and consequently, its contribution to the conduction g-tensor is by no means dominating. Therefore, we attempt to do a more careful analysis. We still work with the effective mass approximation in evaluating the g-tensor, but we use OPW crystal wave functions to calculate all the matrix elements involved in the effective mass formalism. With the exception of the transverse component of the g-tensor in Ge, excellent agreement with experiment is achieved. Since effective mass parameters are involved in the g-tensor calculation, we also include a section to discuss their evaluation from OPW wave functions.

The spin resonance line-width in semiconductors is largely due to a spin-lattice relaxation. Roth[9] has

proposed a spin-lattice relaxation mechanism for Si, which is caused by the modulation of the single valley g-tensor by strain. Using the measured value for a parameter in the proposed mechanism, we evaluate a certain shear deformation-potential matrix element. The result is compared with another deformation-potential matrix element obtained either from conductivity measurement or from measurement of spin-lattice relaxation rate due to a second mechanism proposed by Roth[4] and by Hasegawa[10] independently.

Part of the work on Si has been reported elsewhere.[11]

II. SPIN-ORBIT SPLITTING OF ATOMIC STATES

It is our aim to treat in this section the s-o splitting of atomic valence states in a formalism related to the method we adopt later for the crystals so that we can see how the s-o splitting of energy levels differs in the atom and in the crystal.

The one electron Hamiltonian as derived from reducing the Dirac equation to its non-relativistic limit[12] takes the following form

$$\mathcal{H} = \mathcal{H}_o + \mathcal{H}_{s-o}$$

$$\mathcal{H}_o = \frac{p^2}{2m} + V + \frac{\hbar^2}{8m^2c^2}\nabla^2 V$$

$$\mathcal{H}_{s-o} = \frac{\hbar}{4m^2c^2}(\nabla V \times \underset{\sim}{p})\cdot\underset{\sim}{\sigma} \equiv \underset{\sim}{h}\cdot\underset{\sim}{\sigma}$$

The term $\mathcal{H}_{s-o}$ is the s-o coupling in which $\underset{\sim}{\sigma}$ is the Pauli spin operator. For atomic case where the potential V has spherical symmetry, $\mathcal{H}_{s-o}$ takes the familiar form

$$\mathcal{H}_{s-o} = \zeta \underset{\sim}{\ell}\cdot\underset{\sim}{s} \qquad (2.2)$$

where $\underset{\sim}{s} = \frac{\hbar}{2}\underset{\sim}{\sigma}$. The matrix of $\mathcal{H}_{s-o}$ with respect to one electron states specified by quantum number n,j and ℓ is diagonal and has as its elements

$$\langle n,j,\ell | \mathcal{H}_{s-o} | n,j,\ell \rangle = \zeta_{n\ell} \langle \underset{\sim}{\ell} \cdot \underset{\sim}{s} \rangle_{j,\ell}$$

with

$$\zeta_{n\ell} = \frac{1}{2m^2c^2} \int_0^\infty P_{n\ell}^2 \frac{1}{r} \frac{dV}{dr} \, dr, \qquad (2.3)$$

where $P_{n\ell/r}$ is the radial wave function for the state, and is normalized according to $\int_o^\infty P_{n\ell}^2 \, dr = 1$.

The atomic H-F wave functions have been calculated for many substances. With the tabulated wave functions we can evaluate numerically the one electron s-o coupling strength by (2.3). However, for atomic valence states we choose to take a different approach here. The valence radial wave function $P_{n\ell}$ can be represented by a smooth function which is orthogonalized to all the occupied core states with the same symmetry

$$P_{n\ell} = N\left[\sqrt{\frac{(2a)^{2n'+1}}{(2n')!}} \, r^{n'} e^{-ar} - \sum_t B_t P_{t\ell}\right] \qquad (2.4)$$

where N is a normalization factor and n' and a are two adjustable parameters. The coefficients B_t, as determined by the requirement that $P_{n\ell}$ be orthogonal to the

core states, is

$$B_t = \sqrt{\frac{(2a)^{2n'+1}}{(2n')!}} \int_o^\infty P_{t\ell} r^{n'} e^{-ar} dr \qquad (2.5)$$

In the core region, the wave function $P_{n\ell}$ in (2.4) is dominated by its core terms; if we are to calculate the s-o integral $\zeta_{n\ell}$ in (2.3) by using the wave function in (2.4), we can neglect the smooth part. Then the s-o splitting $\Delta_{n\ell}$ of the one electron valence state can be expressed in terms of that of the core states as

$$\Delta_{n\ell} = N^2 \sum_t B_t^2 \Delta_{t\ell} + N^2 \sum_{t,t'} B_t B_{t'} \times (\langle \underset{\sim}{\ell} \cdot \underset{\sim}{s} \rangle_{j=\ell+\frac{1}{2},\ell}$$

$$- \langle \underset{\sim}{\ell} \cdot \underset{\sim}{s} \rangle_{j'=\ell-\frac{1}{2},\ell}) \times \frac{1}{2m^2c^2} \int_o^\infty P_{t\ell} P_{t'\ell} \frac{1}{r} \frac{dV}{dr} dr \qquad (2.6)$$

The second term is usually smaller than the first one.

For neutral Ge, the atomic H-F wave functions have been calculated by Piper.[13] We use his tabulated wave functions for $P_{n\ell}$ in (2.3) and also for constructing the atomic potential V to obtain the atomic s-o splitting for the various states. The atomic potential V is assumed to be pure Coulomb potential. Then, $\frac{dV}{dr}$ in (2.3) can be obtained from the tabulated radial wave functions by

$$\frac{dV}{dr} = \frac{e}{r^2} \left[Z - \sum_{n,\ell} w_{n\ell} \int_o^r P_{n\ell}^2(r) dr \right] \qquad (2.7)$$

where Z is the atomic number and $w_{n\ell}$ is the number of electrons occupying the state specified by quantum number n and ℓ. The summation is extended over all occupied states.

The calculated splittings for the core states are listed in Tabe I together with the core splitting for Si. The calculated value for the atomic 4p splitting is $\Delta_{4p} = 0.15$ ev. This is to be compared with the experimental value of $\Delta_{4p} = 0.18$ ev deduced from spectroscopic term values with a configuration of $4s^2 4p^2\ ^3P$;[14] the experimental value is about 20% greater than the calculated value. On the other hand, we can fit Piper's tabulated wave function reasonably well by (2.4) with the following values for the parameters.

$$\begin{aligned} N &= 1.002 \\ n' &= 4 \\ a &= 1.85 \\ B_{2p} &= .006520 \\ B_{3p} &= -.1987 \end{aligned} \qquad (2.8)$$

Then, from (2.6), (2.8) and core splittings in Table I we obtain $\Delta_{4p} = 0.15$ ev, which is exactly the value obtained from the original tabulated 4p function. The 2p - 3p interference term (second term in (2.6)) in

Δ_{4p} amounts to 0.01 ev.

In our later discussion of the crystal case, we shall evaluate the band s-o splitting for Ge at the center of the B.Z. We are then going to compare the crystal result with the atomic result obtained by (2.6). Through this explicit comparison we hope to illustrate the enhancement of the s-o splitting above atomic values found experimentally in certain crystals.

III. SPIN-ORBIT SPLITTING OF ENERGY BANDS

In the framework of the one electron theory, the Hamiltonian for an electron in a crystal is given by (2.1). It is well known that the eigenstates of $\mathcal{H}_o$ are represented by Bloch functions and the energy eigenvalues form bands in the B.Z. due to the periodicity of the crystal potential V. There are different methods for calculating eigenfunctions of $\mathcal{H}_o$ in practical cases, but by far the most successful method for getting valence state wave functions in semiconductors is the OPW method. The crystal valence wave functions in terms of OPW's may be separated into a 'smooth' plane wave part and a core part similar to the atomic valence function (2.4)

$$\psi_{\underset{\sim}{k}}^{\alpha} = \sum_{\underset{\sim}{K}} a(|\underset{\sim}{k}+\underset{\sim}{K}|)\,|(\underset{\sim}{k}+\underset{\sim}{K})\rangle^{\alpha} + \sum_{t} b_{\underset{\sim}{k},t}^{\alpha}\,|\phi_{\underset{\sim}{k},t}{}^{\alpha}\rangle \qquad (3.1)$$

Here α is a symbol for the irreducible representation used to denote the symmetry of the wave function, $\underset{\sim}{k}$ is the wave vector and $\underset{\sim}{K}$ is the reciprocal lattice vector. Plane waves are expressed by $(\underset{\sim}{k}+\underset{\sim}{K})$. The symbol $|\rangle^{\alpha}$ denotes a properly normalized symmetrized combination of plane waves. The second term in (3.1)

is the core part, which comes from orthogonalization and takes the following form

$$\phi_{\underset{\sim}{k},t}^{\alpha} = \frac{1}{\sqrt{sN}} \sum_{\underset{\sim}{R}_n} \sum_{\underset{\sim}{d}} e^{i\underset{\sim}{k}\cdot(\underset{\sim}{R}_n+\underset{\sim}{d})} \chi_t^{\alpha}(\underset{\sim}{r}-\underset{\sim}{R}_n-\underset{\sim}{d}) \qquad (3.2)$$

Here χ_t^{α} is the atomic core wave function with symmetry specified by α, $\underset{\sim}{d}$ is the position of the atom with respect to the lattice vector $\underset{\sim}{R}_n$, N in the normalization factor is the number of unit cells in the crystal and s denotes the number of atoms per unit cell. The normalization of the wave function is such that both χ_t^{α} and ψ_k^{α} are normalized to one over the whole crystal.

For some semiconductors, the s-o coupling strength is small compared to the energy gap. In this case, $\mathcal{H}_{s-o}$ in (2.1) can be treated as a perturbation term. Then in order to evaluate the energy band splitting, we must first take matrix elements of $\mathcal{H}_{s-o}$ with respect to states $\psi_{\underset{\sim}{k}}^{\alpha}|\pm\rangle$, where $|+\rangle$ and $|-\rangle$ are the two spin eigenstates of σ_z. An s-o matrix element using $\psi_{\underset{\sim}{k}}^{\alpha}$ in (3.1) can be separated into three parts: namely, the matrix element between two plane wave parts, between a plane wave part and a core part, and between two core parts. The last one gives the most important contribution. For example, in Si the

core-core term is found to be about 96% of the whole matrix element. In Ge, because it has a larger core, the core-core term is even more important. Therefore, for the purpose of evaluating the s-o matrix element, we represent the valence wave function by its core part only. In this way a general matrix element of $\mathcal{H}_{s-o}$ takes the following form:

$$\langle \psi_{\underset{\sim}{k}}^{\alpha\pm} | \mathcal{H}_{s-o} | \psi_{\underset{\sim}{k}}^{\beta\pm} \rangle \propto \sum_{t,t'} b_{\underset{\sim}{k},t}^{\alpha *} b_{\underset{\sim}{k},t'}^{\beta} \langle \chi_t^{\alpha} | h_i | \chi_{t'}^{\beta} \rangle \quad (3.3)$$

To obtain the right hand side of the above equation we have assumed that there is no overlap between the core orbitals centered around different lattice points. The operator h_i in $\langle \chi_t^{\alpha} | h_i | \chi_{t'}^{\beta} \rangle$ is used to denote a definite component of $\underset{\sim}{h}$ determined by the symmetry α and β.

We notice that the matrix element $\langle \chi_t^{\alpha} | h_i | \chi_t^{\beta} \rangle$ is connected with the s-o splitting of the core states. Therefore, the s-o splitting of the crystal valence states like that of the atomic valence state, can be expressed in terms of the splitting of all the occupied core states, the magnitude of which can be obtained either from x ray data or from calculation using a model crystal potential and tabulated atomic wave functions. The coefficients $b_{\underset{\sim}{k},t}^{\alpha}$ can be expressed in terms of the plane wave coefficients $a^{\alpha}(\underset{\sim}{k}+\underset{\sim}{K})$ in (3.1)

and the orthogonalization coefficients $B_t(\underset{\sim}{k}+\underset{\sim}{K})$ used in the usual OPW band calculation:

$$b^{\alpha}_{\underset{\sim}{k},t} = - \sum^{\alpha}_{\underset{\sim}{K}} a(|\underset{\sim}{k}+\underset{\sim}{K}|) B_t(\underset{\sim}{k}+\underset{\sim}{K}) e^{i\underset{\sim}{K}\cdot\underset{\sim}{d}} \qquad (3.4)$$

where α in the summation sign indicates that this is a symmetrized sum for α irreducible representation. From (3.4) it is seen that the magnitude of $(b^{\alpha}_{k,t})^* b^{\beta}_{k,t'}$ in (3.3) depends on the number of terms we take in the expansion into symmetrized combination of OPW's for the valence wave functions. Any truncation of the infinite secular determinents arising in the OPW method not only leads to unavoidable errors to the energy eigenvalues but also to larger errors in the s-o splitting. Therefore in any calculation of the s-o splitting, it is advisable to study the convergence.

In order to illustrate the general procedures outlined above and to make explicit use of the crystal symmetry we take up in the following section diamond type crystals.

IV. DIAMOND TYPE CRYSTALS

There have been extensive studies on the energy bands for crystals with diamond structure. In particular, the band structures without s-o coupling for Si and Ge are sketched in Fig. 1 and Fig. 2 respectively For both substances, the valence edge is at $\Gamma_{25'}$. The conduction edge for Si lies at $\underset{\sim}{k}_o = (\Delta,0,0)$ along Δ_1 with $\Delta = 0.85 \frac{2\pi}{a}^{15}$, and that for Ge lies at L_1. For these substances, $\mathcal{H}_{s-o}$ in (2.1) can be treated as a perturbation term. Therefore, using the method outlined in the above section, we try to evaluate the splitting of the valence states at positions in the B.Z. corresponding to both the valence edge and to the conduction edge, or at $\Gamma_{25'}$ and Δ_5 for Si and $\Gamma_{25'}$ and $L_{3'}$ for Ge.

The diamond structure consists of two interpenetrating face-centered cubic sublattices. We take as the origin of our coordinate system a point midway between two adjacent lattice points and distinguish

the core orbitals in (3.2) centered around the two sublattices by a superscript 1 or 2 and denote the valence wave function by its core part only. In accordance with these conventions we list in the following some useful wave functions

$$\Gamma_{25'}^{xy} = b_{2p}^{\Gamma_{25'}}(\phi_{2z}{}^{1}-\phi_{2z}{}^{2}) + b_{3p}^{\Gamma_{25'}}(\phi_{3z}{}^{1}-\phi_{3z}{}^{2}) + b'^{\Gamma_{25'}}_{3d}(\phi_{xy}{}^{1}+\phi_{xy}{}^{2}) \tag{4.1}$$

$$\Delta_5{}^{y} = b_{2p}^{\Delta_5}(\phi_{2z}{}^{1}-\phi_{2z}{}^{2}) + b'^{\Delta_5}_{2p}(\phi_{2y}{}^{1}+\phi_{2y}{}^{2}) + b_{3p}^{\Delta_5}(\phi_{3z}^{1}-\phi_{3z}^{2}) + b'^{\Delta_5}_{3p}(\phi_{3y}{}^{1}+\phi_{3y}{}^{2}) + b_{3d}^{\Delta_5}(\phi_{zx}{}^{1}-\phi_{zx}{}^{2}) + b'^{\Delta_5}_{3d}(\phi_{yx}{}^{1}+\phi_{yx}{}^{2}) \tag{4.2}$$

$$L_{3'}{}^{y'} = b'^{L_{3'}}_{2p}(\phi^{1}_{2y',+}+\phi^{2}_{2y',-}) - (b'^{L_{3'}}_{2p})^{*}(\phi^{1}_{2y',-}+\phi^{2}_{2y',+}) + b'^{L_{3'}}_{3p}(\phi^{1}_{3y',+}+\phi^{2}_{3y',-}) - (b'^{L_{3'}}_{3p})^{*}(\phi^{1}_{3y',-}+\phi^{2}_{3y',+})$$

$$+ b_{3d,y'z'}^{L_{3'}}(\phi_{y'z',+}^{1}-\phi_{y'z',-}^{2}) - (b_{3d,y'z'}^{L_{3'}})^{*}(\phi_{y'z',-}^{1}-\phi_{y',+}^{2})$$

$$+ b_{3d,y'x'}^{L_{3'}}(\phi_{y'x',+}^{1}-\phi_{y'x',-}^{2}) - (b_{3d,y'x'}^{L_{3'}})^{*}(\phi_{y'x',-}^{1}-\phi_{y'z',+}^{2}),$$

$$L_{3'}{}^{z'} = b_{2p}^{L_{3'}}(\phi_{2z',+}^{1}+\phi_{2z',-}^{2}) - (b_{2p}^{L_{3'}})^{*}(\phi_{2z',-}^{1}+\phi_{2z',+}^{2})$$

$$+ b_{2p}^{L_{3'}}(\phi_{3z',+}^{1}+\phi_{3z',-}^{2}) - (b_{3p}^{L_{3'}})^{*}(\phi_{3z',-}^{1}+\phi_{3z',+}^{2})$$

$$+ b_{3d,y'z'}^{L_{3'}}(\phi_{y',2-z',2,+}^{1}-\phi_{y',2-z',2,-}^{2})$$

$$- (b_{3d,y'z'}^{L_{3'}})^{*}(\phi_{y',2-z',2,-}^{1}-\phi_{z'x',+}^{2})$$

$$+ b_{3d,y'x'}^{L_{3'}}(\phi_{z'x',+}^{1}-\phi_{z'x',-}^{2})$$

$$- (b_{3d,y'x'}^{L_{3'}})^{*}(\phi_{z'x',-}^{1}-\phi_{z'x',+}^{2}) \qquad (4.3)$$

We have used the irreducible representation symbols to denote the wave functions with superscripts specifying the symmetry type. The wave functions $L_{3'}$ are expressed in terms of primed coordinates in which x' refers to the (1,1,1) direction. We have omitted the subscript $\underset{\sim}{k}$ of $\phi_{\underset{\sim}{k}}$ in (4.1) and (4.2), but in (4.3) we have used the subscripts + or - to specify $\underset{\sim}{k}$ being

$(\frac{1}{2},\frac{1}{2},\frac{1}{2})\frac{2\pi}{a}$ or $-(\frac{1}{2},\frac{1}{2},\frac{1}{2})\frac{2\pi}{a}$. It is also to be noted that we have only included core states up to the atomic 3d state in the wave functions. Some of the coefficients b and b' will later be given explictly in terms of $a(|\underset{\sim}{k}+\underset{\sim}{K}|)$, and $B_t(\underset{\sim}{k}+\underset{\sim}{K})$.

At $\Gamma_{25'}$

The valence state $\Gamma_{25'}$ is six fold degenerate (spin degeneracy included). When we treat $\mathcal{H}_{s-o}$ as a perturbation on $\mathcal{H}_o$ in (2.1), we only take into consideration the three degenerate orbital states, one of which is given explictly in (4.1), and the two spin eigenstates $|+\rangle$ and $|-\rangle$ of σ_z. With respect to these states, the only nonvanishing matrix elements of $\mathcal{H}_{s-o}$ are:

$$\langle \Gamma_{25'}^{xy},\pm|\mathcal{H}_{s-o}|\Gamma_{25'}^{yz},\mp\rangle = \mp i\Big[\,|b_{2p}^{\Gamma_{25'}}|^2\langle\chi_{2z}|h_y|\chi_{2x}\rangle + |b_{3p}^{\Gamma_{25'}}|^2\langle\chi_{3z}|h_y|\chi_{3x}\rangle + 2(\mathrm{Re}(b_{2p}^{\Gamma_{25'}})^* b_{3p}^{\Gamma_{25'}}) \times \langle\chi_{2z}|h_y|\chi_{3x}\rangle - |b_{3d}^{\Gamma_{25'}}|^2\langle\chi_{yz}|h_y|\chi_{xy}\rangle\Big]$$

$$\equiv \mp iS \quad , \tag{4.4}$$

$\langle \Gamma_{25'}^{xy},\pm|\mathcal{H}_{s-o}|\Gamma_{25'}^{zx},\mp\rangle$, and $\langle \Gamma_{25'}^{yz},\pm|\mathcal{H}_{s-o}|\Gamma_{25'}^{zx},\pm\rangle$

together with their complex conjugates. The Hamiltonian is then a 6×6 matrix:

$$\begin{pmatrix} 0 & 0 & 0 & 0 & -iS & -S \\ 0 & 0 & S & -iS^* & 0 & 0 \\ 0 & S^* & 0 & -S^* & 0 & 0 \\ 0 & iS & -S & 0 & 0 & 0 \\ iS^* & 0 & 0 & 0 & 0 & S \\ -S^* & 0 & 0 & 0 & S^* & 0 \end{pmatrix} \tag{4.5}$$

This matrix can be reduced to two identical 3×3 matrices. In other words, the s-o split levels are at least doubly degenerate. This Kramer's degeneracy is due to space inversion and time reversal symmetry of the Hamiltonian. After diagonalization of the Hamiltonian, we see that the $\Gamma_{25'}$ state splits into two, for which the energy shifts are:

$$\Delta E_1 = iS \qquad \text{(quartic degenerate)}$$

and

$$\Delta E_2 = -2iS \quad \text{(doubly degenerate)} \tag{4.6}$$

Since most of the s-o matrix elements in S are connected with the atomic core s-o splittings, the valence s-o splitting in the crystal can be conveniently obtained

through the splitting of the core states Δ_{2p}, Δ_{3p} and Δ_{3d} as follows

$$\Delta_{s-o}(\Gamma_{25'}) = |b_{2p}^{\Gamma_{25'}}|^2 \Delta_{2p} + |b_{3p}^{\Gamma_{25'}}|^2 \Delta_{3p} - \frac{3}{5}|b_{3d}^{\Gamma_{25'}}|^2 \Delta_{3d}$$

$$+ 6(R_e(b_{2p}^{\Gamma_{25'}})^* b_{3p}^{\Gamma_{25'}}) \langle \chi_{2z}|h_y|\chi_{3x}\rangle \quad (4.7)$$

According to (3.4), the coefficient b's in terms of plane wave and orthogonalization coefficients are equal to

$$b_{2p,3p}^{\Gamma_{25'}} = i\left[\frac{2}{\sqrt{3}} a^{\Gamma_{25'}}(\sqrt{3})\, B_{2p,3p}(\sqrt{3}) + \sqrt{2}\, a^{\Gamma_{25'}}(2) B_{2p,3p}(2) + \ldots\right]$$

$$b_{3d}^{\Gamma_{25'}} = \frac{2}{\sqrt{3}} a^{\Gamma_{25'}}(\sqrt{3})\, B_{3d}(\sqrt{3}) + \sqrt{3}\, a^{\Gamma_{25'}}(2\sqrt{2})\, B_{3d}(2\sqrt{2}) + \ldots. \quad (4.8)$$

Here we have used orthogonalization coefficients which depend only on the magnitude $|\underset{\sim}{k}+\underset{\sim}{K}|$ of the wave vectors, given in units of $2\pi/a$ in the argument of B_t. The variation of $B_t(\underset{\sim}{k}+\underset{\sim}{K})$ with the directions of a set of wave vectors of the same magnitude has been absorbed into the numerical factors in (4.8).

In any quantitative evaluation of the splitting of $\Gamma_{25'}$ according to (4.7), we first need the splitting of the core states. This can be obtained either

from experimental x ray data or from calculation. On the experimental side, Tomboulian and Cady[16] have completed the identification of the x ray emission lines $2p^{3/2} \rightarrow 2s$ and $2p^{\frac{1}{2}} \rightarrow 2s$ for the second row of the periodic table. Their value for the 2p s-o splitting of Si is listed in the first line of Table I. By invoking Slater's rule that the missing electron gives an extra screening charge of 0.3 ev, we can use Tomboulian and Cady's values to estimate the 2p splitting in neutral Si (second line of Table I). As for Ge, there is only an experimental value for the 2p core s-o splitting by Tyren[17] from K-emission data. This value and the corrected value for neutral Ge are also listed.

On the other hand, to calculate the core s-o splitting we assume that the crystal potential has spherical symmetry in the vicinity of each atomic site. Then, its value can be obtained by (2.3). We have already done this for Ge in Section II and we calculate now the 2p core splitting for Si based on crystal potential and atomic core wave functions used by Kleinman and Phillips[18] in their Si band calculation. All the calculated results are listed in Table I. In all the subsequent calculations we shall use the corrected experimental value for the Si 2p core s-o splitting and the calculated values for the three Ge core (2p, 3p and 3d states) splittings.

To obtain the plane wave and orthogonalization coefficients for the evaluation of $b^{\Gamma_{25'}}_{2p,3p}$ and $b'^{\Gamma_{25'}}_{3d}$ in (4.8) for Si, we rely upon K and P's crystal wave functions. For Ge, we use the H-F atomic wave function by Piper[13] and a computer program furnished by F. Bassani and M. Yoshimine to run the Ge OPW crystal wave function on an IBM 704 computer. We include in the appendix a brief discussion on this calculation and a list of the orthogonalization and plane wave coefficients. The corresponding Si values may be obtained from K and P.

With the core splittings and coefficients b and b', we evaluate the s-o splitting of the $\Gamma_{25'}$ state for Si and Ge by successively taking more and more plane waves in (4.8). The convergence of the calculation is shown in Fig. 3. After about 80 plane waves the calculated splitting is expected to change by no more than 7%, because the plane wave coefficients for any higher $\underset{\sim}{K}$ are very small. This expectation is represented by dotted lines in Fig. 3 indicating approximate convergence. In the study of convergence, we have neglected the contribution from 2p - 3p interference term in (4.7) to Δ^{Ge}_{s-o}; this is to be corrected in the final result. The s-o splittings for Ge and Si thus obtained are $\Delta^{Si}_{s-o}(\Gamma_{25'}) = 0.042$ ev and

$\Delta^{Ge}_{s-o}(\Gamma_{25'}) = 0.29$ ev. They are to be compared with the experimental values of $\Delta^{Si}_{s-o}(\Gamma_{25'}) = 0.0441 \pm .0004$ ev[7] and $\Delta^{Ge}_{s-o}(\Gamma_{25'}) = 0.3$ ev.[8] The agreement in both cases is good. In the calculation for $\Delta^{Ge}_{s-o}(\Gamma_{25'})$ we find that the 3d state contributes only 2% (of opposite sign to the contribution from p states) and the 2p state 4% to this value.

As $\Gamma_{25'}$ is of atomic p symmetry type, we compare $\Delta^{Ge}_{s-o}(\Gamma_{25'})$ with Δ^{Ge}_{4p} of Section II. We notice that according to calculations the splitting in crystal is about 2 times larger than that in the atom. To see how this enhancement comes about we compare $b_t^{\Gamma_{25'}}$ of (4.8) with NB_{2p} in (2.6). The average value of the orthogonalization coefficients $B_t(|\underset{\sim}{k}+\underset{\sim}{K}|)$ in $b_t^{\Gamma_{25'}}$ is about the same in magnitude as the corresponding B_t for the atomic wave function. However the rest of $b_t^{\Gamma_{25'}}$, which is essentially a summation of plane wave coefficients, adds up to 1.78 for about 80 plane waves in (4.8) while in the atomic case N = 1.02. Physically, this difference in normalization constants means that the wave function in crystal gets contracted in the core region of each atomic site. It is this contraction which gives rise to an enhancement of the s-o splitting. For Si, the same enhancement is noticed; the atomic splitting $\Delta^{Si}_{3p} = 0.028$ ev from spectroscopic

term values[14] with the configuration $3s^2\ 3p^2\ {}^3P$. Since at present there are no atomic H-F wave functions calculated for neutral Si, it is not possible to carry out a calculation similar to what we did for Ge in Section II to demonstrate the enhancement.

Along Δ_5 for Si

The s-o splitting of the energy bands along Δ_5 in diamond structure solids has been qualitatively discussed by Englert.[19] Although he uses tight-binding type wave functions while we use OPW crystal wave functions, the qualitative features of our results are the same since they all depend on the crystal symmetry only.

For simplicity we consider explicitly the case for Si in this section. We first consider the region near the zone edge X_4 and then the region near $\Gamma_{25'}$. In the former region, we are far away from the zone center. Then in studying the s-o splitting of the Δ_5 valence band, we only need take the two degenerate states $\Delta_5{}^y$ and $\Delta_5{}^z$ into consideration, one of which is given in (4.2). With respect to these states, the only nonvanishing matrix elements of $\mathcal{H}_{s-o}$ are:

$$\langle \Delta_5{}^y \pm | \mathcal{H}_{s-o} | \Delta_5{}^z \rangle = (|b'^{\Delta_5}_{2p}|^2 - |b^{\Delta_5}_{2p}|^2) \times \langle \chi_{2y} | h_x | \chi_{2z} \rangle \qquad (4.9)$$

and their complex conjugates. Then, the degenerate Δ_5 state splits into two states, each doubly degenerate (Kramer's degeneracy), and the splitting is equal to

$$\Delta^{Si}_{s-o}(\Delta_5) = \frac{2}{3}\left[\left|b'^{\Delta_5}_{2p}\right|^2 - \left|b^{\Delta_5}_{2p}\right|^2\right] \Delta^{Si}_{2p} \qquad (4.10)$$

In terms of parameters in OPW type band calculations, the coefficients $b^{\Delta_5}_{2p}$ and $b'^{\Delta_5}_{2p}$ are:

$$b^{\Delta_5}_{2p} = \sqrt{2}\, i\left[\frac{1}{\sqrt{\delta^2+2}}\, a^{\Delta_5}(\sqrt{\delta^2+2})\; B_{2p}(\sqrt{\delta^2+2}) + \frac{2}{\sqrt{(\delta+1)^2+4}}\; a^{\Delta_5}(\sqrt{(\delta+1)^2+4})\; B_{2p}(\sqrt{(\delta+1)^2+4})+\ldots\right]$$

$$b'^{\Delta_5}_{2p} = -\sqrt{2}\left[\frac{1}{\sqrt{\delta^2+2}}\, a^{\Delta_5}(\sqrt{\delta^2+2})\; B_{2p}(\sqrt{\delta^2+2}) + \frac{2}{\sqrt{(\delta-1)^2+4}}\; a^{\Delta_5}(\sqrt{(\delta-1)^2+4})\; B_{2p}(\sqrt{(\delta-1)^2+4})+\ldots\right] \qquad (4.11)$$

using the direction independent orthogonalization coefficients as in (4.8). Here $(\delta+1,0,0)$ is the position in the B.Z. under consideration in units of $2\pi/a$. According to the terms listed in (4.11), the difference in $|b^{\Delta_5}_{2p}|$ and $|b'^{\Delta_5}_{2p}|$ is due to one containing the $(\delta+1,2,0)$ set of plane waves and the other the $(\delta-1,2,0)$ set. The first thing to be noted

is that at $X_4(\delta=0)$, $|b_{2p}{}^{\Delta_5}|$ is equal to $|b'_{2p}{}^{\Delta_5}|$. Then, according to (4.10)

$$\Delta^{Si}_{s-o}(X_4) = 0 \quad , \tag{4.12}$$

which is consistent with the prediction by Elliott[1] using the theory of the double group. Next, we go away from X_4 toward the zone center but keep $|\delta|$ small. By (4.10) and (4.11), the s-o splitting of the Δ_5 state reflects the properties of the wave functions through the difference between $b_{2p}{}^{\Delta_5}$ and $b'_{2p}{}^{\Delta_5}$. However, the orthogonalization coefficients and the numerical factors in $|b_{2p}{}^{\Delta_5}|$ and $|b'_{2p}{}^{\Delta_5}|$ are not sensitive functions of k; their product only changes about 1% when $|\delta|$ changes from 0 to 0.5. Therefore, the difference is mainly due to the coefficients a^{Δ_5}. The secular determinants for Δ_5 and X_4 in the OPW method have identical off-diagonal elements; only their diagonal elements $\frac{\hbar^2}{2m}(\underset{\sim}{k}+\underset{\sim}{K})^2$ differ. Therefore, by using perturbation technique, we can establish that

$$a^{\Delta_5}(\sqrt{(\delta+1)^2+4}) = a^{X_4}(\sqrt{5})\ (1+\tfrac{2}{3}|\delta|)$$

$$a^{\Delta_5}(\sqrt{(\delta-1)^2+4}) = a^{X_4}(\sqrt{5})\ (1-\tfrac{2}{3}|\delta|), \tag{4.13}$$

when δ is small. It is then evident from (4.10) that $\Delta_{s-o}(\Delta_5)$ is proportional to $|\delta|$ if higher order terms are neglected. To determine the proportionality constant, we calculate the s-o splitting of Δ_5 at the conduction band edge $\underset{\sim}{k}_o$ for Si (δ=-0.15 at $\underset{\sim}{k}$). The calculation using the band parameters of K and P establishes that

$$\Delta^{Si}_{s-o}(\Delta_5) = 0.17|\delta|\Delta^{Si}_{s-o}(\Gamma_{25'}) \quad , \qquad \text{(near } X_4\text{)} \tag{4.14}$$

where δ is in units of $2\pi/a$ as before.

We now go to the region in the vicinity of $\underset{\sim}{k} = 0$. First we would like to mention that although there is a splitting for $\Gamma_{25'}$, the lower doubly degenerate level goes to Δ_7 (in the notation of the double group) associated with the orbital state $\Delta_{2'}$. So, as far as the orbital state Δ_5 is concerned, the splitting is zero at the zone center. In the vicinity of $\underset{\sim}{k} = 0$, we have to take the $\Delta_{2'}$ state into consideration when studying the s-o splitting of Δ_5. The conduction state Δ_1 does not have much influence since the conduction-valence energy gap is about 30 times larger than the Δ_5 s-o splitting. Using the three states Δ_5^y, Δ_5^z, and $\Delta_{2'}$ as a basis we diagonalize the s-o Hamiltonian and get the energy shift for

the Δ_5 level as:

$$\Delta^{Si}_{s\text{-}o}(\Delta_5) = \tfrac{1}{2}\Big|E_{\Delta_5} - E_{\Delta_{2'}} + \Delta^{Si}_{s\text{-}o}(\Gamma_{25'}) - \sqrt{(E_{\Delta_5} - E_{\Delta_{2'}} + \frac{\Delta^{Si}_{s\text{-}o}(\Gamma_{25'})}{3})^2 + \frac{8}{9}\Delta^{Si\,2}_{s\text{-}o}(\Gamma_{25'})}\Big| \quad \text{(near } \Gamma_{25'}\text{)} \quad (4.15)$$

In getting (4.15), we have assumed that all band parameters appropriate to small $\underset{\sim}{k}$ are given by those at $\underset{\sim}{k} = 0$. Furthermore, in the vicinity of $\underset{\sim}{k} = 0$, E_{Δ_5} and $E_{\Delta_{2'}}$ are given in terms of hole effective mass parameters[20,21] so that

$$E_{\Delta_5}(k) - E_{\Delta_{2'}}(k) = (M-L)k^2 \qquad (4.16)$$

The values of M and L for Si as deduced from experiments[18,22] are M = -6.1 and L = -2.8 in units of $\hbar^2/2m$. Therefore, we can use (4.15) to get a quantitative estimate of the s-o splitting for Δ_5 near the center of the B.Z.

In summary, we see that at the zone center, the s-o splitting for Δ_5 is equal to zero. As we move away from the center, the splitting increases and then decreases to zero again at the zone edge. A sketch of $\Delta^{Si}_{s\text{-}o}(\Delta_5)$ vs. k_x is given in Fig. 4.

At $L_{3'}$ and Along Λ_3 for Ge

To evaluate the s-o splitting at $L_{3'}$ for Ge, we still treat $\mathcal{H}_{s-o}$ as a perturbation on the doubly (orbital) degenerate state $L_{3'}$, the wave functions of which are given in (4.3). The calculated results vs. number of plane waves taken for the basis functions is again shown in Fig. 3. We take as our calculated result $\Delta^{Ge}_{s-o}(L_{3'}) = 0.18$ ev after putting in correction due to 2p - 3p cross term. The most recent experimental value from a reflectivity measurement by Cardona and Sommers[8] is $\Delta^{Ge}_{s-o}(L_{3'}) = 0.18$ ev. In the calculation, we find again as in the calculation for $\Delta^{Ge}_{s-o}(\Gamma_{25'})$ that the most important state which contributes to the valence state (both $\Gamma_{25'}$ and $L_{3'}$) splitting of Ge is the 3p core state. The 3d state contributes a value of less than 1% and 2p a value of about 4% of the total splitting. These facts are readily understandable. First, the 3d state is not important because there should not be too much d character in the crystal valence states we are considering, which evolve mainly from the atomic 4p state. Second, the 2p state does not contribute appreciably because it has a small radius, resulting in small values for the 2p orthogonalization coefficients B_{2p}.

Next, we discuss qualitatively the behaviour of

the s-o splitting of Λ_3 in going from Γ_{25}, to $L_{3'}$ along the (111) axis in the B.Z. In examining (4.1) and (4.3) we see that Γ_{25}, contains bonding p character (antibonding d character), or $\phi_p^1 - \phi_p^2$ type wave functions while $L_{3'}$ contains antibonding p character (bonding d character), or $\phi_p^1 + \phi_p^2$ type wave functions. Along Λ_3 there is no inversion symmetry in the group of the k vector; hence, both bonding and antibonding types are allowed in the wave function. Somewhere along Λ_3, the weight of the two types must be equal. Then, according to procedures which lead to (4.10), the s-o splitting should vanish at this point. This shows that the s-o split levels along Λ_3 have a cross-over. We shall see in Section V that under a two band approximation the longitudinal g-tensor for conduction electrons in Si is related to the s-o splitting of the Δ_5 valence state and is larger than the free electron g-value 2.0023. When we go from Δ_5 to $L_{3'}$, we encounter a cross-over in the s-o split levels. Since the s-o splitting at $L_{3'}$ is related to the longitudinal g-tensor for conduction electrons in Ge, it becomes smaller than 2.0023 under a two level assumption which is consistent with experiments.

V. g-Tensor

As we have seen in the last section, there exists a Kramer's degeneracy in the energy bands of diamond type crystals even with s-o interaction. However, if we put the crystals under a magnetic field of strength H, the two fold degeneracy is lifted. The Hamiltonian in (2.1) then has an additional term

$$\mathcal{H}_m = \tfrac{1}{2}\beta \, \underset{\sim}{\sigma} \cdot \underset{\sim}{\underset{\sim}{g}} \cdot \underset{\sim}{H} \qquad (5.1)$$

where β is the Bohr magneton. In the absence of s-o interaction, g becomes a scalar quantity and is equal to 2.0023. On the other hand, in addition to a diamagnetic contribution, the orbital motion of the electron under a magnetic field changes the value of g from 2.0023 through s-o coupling. For some semiconductors when the conduction band edges consist of several valleys and lie along symmetry axis instead of at the origin of the B.Z., the electron energy surface may no longer be a sphere even if the crystal possesses cubic symmetry. In this case, s-o interaction introduces anisotropy into the g-value and

makes it a tensorial quantity as indicated in (5.1). To obtain in theory the dependence of $\underset{\sim}{g}$ on the details of the orbital motion of Bloch electrons is in general a difficult task because the magnetic interaction can not be treated as a perturbation on Bloch states which have a quasi-continuous energy spectrum. For Na, Yafet[2] used a cellular method to solve numerically the magnetic Schrodinger equation to obtain the g-factor. For paramagnetic ions embedded in crystalline salts, we abandon the band picture and regard the electron as localized at the ion position. Then, with respect to the discrete atomic states, the electronic interaction with crystalline field and magnetic field can be treated by perturbation theory. This localized electron picture does not apply to conduction electrons in semiconductors. Nevertheless, since only states in the immediate vicinity of band edges are important, we can ignore the $\underset{\sim}{k}$ dependence of the g-tensor and use the effective mass approximation. In this approximation, general formula for the g-tensor are contained in several papers[4,5] and need not be repeated here. For some semiconductors like Si and Ge, details of energy band structure are known and use can be made of the symmetry properties of various states to obtain selection rules for the matrix elements involved in

the effective mass formalism. In this way Roth derived the following formula for the g-shift of conduction electrons in Si and Ge by treating $\mathcal{H}_{s-o}$ as a perturbation.

$$\delta g_{\parallel}^{Si} = \delta g_{x}^{Si} = \mathrm{Re}\,\frac{4}{mi}\sum_{\mu,\nu}\frac{1}{E_{o\mu}E_{o\nu}}\langle\Delta_1|P_y|\Delta_5^{\mu y}\rangle\langle\Delta_5^{\mu y}|h_x|\Delta_5^{\nu z}\rangle$$

$$\times\ \langle\Delta_5^{\nu z}|P_z|\Delta_1\rangle$$

$$+\ \mathrm{Re}\,\frac{8}{mi}\sum_{\mu,\nu}\frac{1}{E_{o\mu}E_{o\nu}}\langle\Delta_1|h_x|\Delta_1^{\mu},\rangle\langle\Delta_1^{\mu},|P_y|\Delta_5^{\nu z}\rangle$$

$$\times\ \langle\Delta_5^{\nu z}|P_z|\Delta_1\rangle\ ,$$

$$\delta g_{\perp}^{Si} = \delta g_{y,z}^{Si} = \mathrm{Re}\,\frac{4}{mi}\sum_{\mu,\nu}\frac{1}{E_{o\mu}E_{o\nu}}\langle\Delta_1|P_z|\Delta_5^{\mu z}\rangle\langle\Delta_5^{\mu z}|h_y|\Delta_1^{\nu}\rangle$$

$$\times\ \langle\Delta_1^{\nu}|P_x|\Delta_1\rangle$$

$$+\ \mathrm{Re}\,\frac{4}{mi}\sum_{\mu,\nu}\frac{1}{E_{o\mu}E_{o\nu}}\langle\Delta_1|h_y|\Delta_5^{\mu z}\rangle\langle\Delta_5^{\mu z}|P_z|\Delta_1^{\nu}\rangle$$

$$\times\ \langle\Delta_1^{\nu}|P_x|\Delta_1\rangle$$

$$+\ \mathrm{Re}\,\frac{4}{mi}\sum_{\mu,\nu}\frac{1}{E_{o\mu}E_{o\nu}}\langle\Delta_1|P_z|\Delta_5^{\mu z}\rangle\langle\Delta_5^{\mu z}|P_x|\Delta_5^{\nu z}\rangle$$

$$\times\ \langle\Delta_5^{\nu z}|h_y|\Delta_1\rangle\ , \qquad (5.2)$$

and

$$\delta g_{\parallel}^{Ge} = \delta g_{x'}^{Ge} = \mathrm{Re}\,\frac{4}{mi}\sum_{\mu,\nu}\frac{1}{E_{o\mu}E_{o\nu}}\langle L_1|P_{y'}|L_3^{\mu y'}\rangle\langle L_3^{\mu y'}|h_{x'}|L_3^{\nu z'}\rangle$$

$$\times\langle L_3^{\nu z'}|P_{z'}|L_1\rangle$$

$$+\,\mathrm{Re}\,\frac{8}{mi}\sum_{\mu,\nu}\frac{1}{E_{o\mu}E_{o\nu}}\langle L_1|h_{x'}|L_2^{\mu}\rangle\langle L_2^{\mu}|P_{y'}|L_3^{\nu z'}\rangle$$

$$\times\langle L_3^{\nu z'}|P_{z'}|L_1\rangle \quad ,$$

$$\delta g_{\perp}^{Ge} = \delta g_{y',z'}^{Ge} = \mathrm{Re}\,\frac{4}{mi}\sum_{\mu,\nu}\frac{1}{E_{o\mu}E_{o\nu}}\langle L_1|P_{z'}|L_3^{\mu z'}\rangle\langle L_3^{\mu z'}|h_{y'}|L_2^{\nu},\rangle$$

$$\times\langle L_2^{\nu},|P_{x'}|L_1\rangle$$

$$+\,\mathrm{Re}\,\frac{4}{mi}\sum_{\mu,\nu}\frac{1}{E_{o\mu}E_{o\nu}}\langle L_1|h_{y'}|L_3^{\mu z'}\rangle\langle L_3^{\mu z'}|P_{z'}|L_2^{\nu},\rangle$$

$$\times\langle L_2^{\nu},|P_{x'}|L_1\rangle$$

$$+\,\mathrm{Re}\,\frac{4}{mi}\sum_{\mu,\nu}\frac{1}{E_{o\mu}E_{o\nu}}\langle L_1|P_{z'}|L_3^{\mu z'}\rangle\langle L_3^{\mu z'}|P_{x'}|L_3^{\nu z'}\rangle$$

$$\times\langle L_3^{\nu z'}|h_{y'}|L_1\rangle \quad . \qquad (5.3)$$

In (5.3), the primed coordinate x' is used to denote the (1,1,1) direction, which is the principal axis of the electron energy ellipsoid in Ge. The expression contains the linear momentum $\underset{\sim}{P}$ matrix elements from

the effective mass approximation and the matrix elements of $\underset{\sim}{h}$ from s-o coupling. See Figs. 1 and 2 for relevent energy levels. Note the core states with superscript "t".

Effective Mass

From the formula for the g-tensor in the effective mass formalism like (5.2) or (5.3), we see that any calculation of the g-tensor involves calculation of s-o and momentum matrix elements. Calculation of s-o matrix elements from OPW crystal wave functions has already been discussed. We now discuss the evaluation of electron effective mass with OPW type wave functions, which involves the calculation of momentum matrix elements.

We rewrite the OPW function in a general form without explicitly specifying its symmetry

$$\psi_{\underset{\sim}{k}} = \sum_{\underset{\sim}{k}} a(\underset{\sim}{k}+\underset{\sim}{K}) \left[\frac{1}{\sqrt{V}} e^{i(\underset{\sim}{k}+\underset{\sim}{K})\cdot \underset{\sim}{r}} - \sum_{t} B_t(\underset{\sim}{k}+\underset{\sim}{K}) \phi_{t,\underset{\sim}{k}+\underset{\sim}{K}} \right] \quad (5.4)$$

where $\phi_{t,\underset{\sim}{k}+\underset{\sim}{K}}$ is defined similar to $\phi^{\alpha}_{t,\underset{\sim}{k}}$ in (3.2) and the normalization is such that the plane wave part of $\psi_{\underset{\sim}{k}}$ is normalized to 1 over the whole space. The momentum matrix element is then evaluated

$$\langle\psi_{\underset{\sim}{k}}|\underset{\sim}{P}|\psi_{\underset{\sim}{k}}\rangle / \langle\psi_{\underset{\sim}{k}}|\psi_{\underset{\sim}{k}}\rangle = \frac{1}{\langle\psi_{\underset{\sim}{k}}|\psi_{\underset{\sim}{k}}\rangle} \times$$

$$\sum_{\underset{\sim}{K},\underset{\sim}{K}'} a^*(\underset{\sim}{k}+\underset{\sim}{K})a(\underset{\sim}{k}+\underset{\sim}{K}')\Big[\hbar(\underset{\sim}{k}+\underset{\sim}{K}) \times$$

$$(\delta_{\underset{\sim}{K},\underset{\sim}{K}'} - 2\sum_t B_t^*(\underset{\sim}{k}+\underset{\sim}{K})B_t(\underset{\sim}{k}+\underset{\sim}{K}'))$$

$$+ \sum_{t,t'} B_t^*(\underset{\sim}{k}+\underset{\sim}{K})B_{t'}(\underset{\sim}{k}+\underset{\sim}{K}')\langle\chi_t|\underset{\sim}{P}|\chi_{t'}\rangle\Big] \qquad (5.5)$$

where

$$\langle\psi_{\underset{\sim}{k}}|\psi_{\underset{\sim}{k}}\rangle = \sum_{\underset{\sim}{K},\underset{\sim}{K}'} a(\underset{\sim}{k}+\underset{\sim}{K})^* a(\underset{\sim}{k}+\underset{\sim}{K}')\Big[\delta_{\underset{\sim}{K},\underset{\sim}{K}'} - \sum_t B_t^*(\underset{\sim}{k}+\underset{\sim}{K})B_t(\underset{\sim}{k}+\underset{\sim}{K}')\Big] \qquad (5.6)$$

Since absolute square of the orthogonalization coefficients is small compared with 1, the last two terms in (5.5) are normally negligible. In addition, the normalization factor in (5.6) may counter-balance the two additional factors due to the core orbitals depending on the sign and the magnitude of the momentum matrix element $\langle\chi_t|\underset{\sim}{P}|\chi_t'\rangle$. This cancellation has been found by K and P in their calculation of the electron and hole effective mass for Si.[18] In a similar calculation for Ge in this section, we hope that this cancellation still prevails. Therefore, we shall take the plane wave part only for the OPW wave function and at the same time neglect the core

contribution to the normalization factor.

The two components of electron effective mass in Ge are given by

$$\left(\frac{m}{m_t^*}\right)_{Ge} = 1 + \frac{2}{m} \sum_{\mu} \frac{1}{E_{o\mu}} |\langle L_1 | P_y, | L_{3'}^{\mu y'} \rangle|^2$$

$$\left(\frac{m}{m_\ell^*}\right)_{Ge} = 1 + \frac{2}{m} \sum_{\mu} \frac{1}{E_{o\mu}} |\langle L_1 | P_x, | L_{2'}^{\mu}, \rangle|^2 \qquad (5.7)$$

A two level approximation is sufficient for the evaluation of (5.7). For m/m_t^* the relevent two levels are the conduction band L_1 and the valence band $L_{3'}$; for m/m_ℓ^* they are L_1 and $L_{2'}^1$, which lies above the conduction band in energy. By using the experimental energy gap value $E_{L_1} - E_{L_{3'}} = 2.1$ ev[23] for m/m_t^* and our calculated gap value $E_{L_1} - E_{L_{2'}^1} = -4.8$ ev for m/m_ℓ^*, the effective mass components are found to be $(m/m_t^*)_{Ge} = 12$ and $(m/m_\ell^*)_{Ge} = 0.52$. Comparing these with the experimental values[24] of $(m/m_t^*)_{Ge} = 12$ and $(m/m_l^*)_{Ge} = 0.61$ from cyclotron resonance, we see that the agreement is satisfactory. Our calculated value -4.8 ev for $E_{L_1} - E_{L_{2'}^1}$ is probably too small in magnitude. A better energy gap value may improve the agreement in the case of $(m/m_\ell^*)_{Ge}$.

Phillips,[15] using the crystal wave function for Ge obtained by his interpolation scheme, evaluated

$(m/m_t^*)_{Ge}$ to be 6.7, or only about one half of the experimental value. It is suspected that this is due to a computational mistake rather than usage of an incorrect value for the energy gap as conjectured by Phillips in his paper.

The Ge hole effective mass parameters have not been calculated here because we are not going to consider the g-factor for holes in this work. The calculation of electron and hole effective mass tensor components for Si has been done by K and P.[18]

Two Band Approximation

From (5.2) and (5.3), we would think it natural that the s-o splitting of the nearby valence band should be responsible for the shift in the g-value of the conduction electron. Then, in theoretical evaluation for the conduction g-tensor, the momentum matrix elements involved can be obtained from the effective mass and the spin-orbit matrix element from the measured splitting of the valence band, or the atomic spin-orbit splitting. Also, the energy gap involved may sometimes be obtained from optical data. In this way, agreement between the estimated g-value and the experimental one provides us with another internal consistency check of the one electron theory. Roth's calculation along this line for $\delta g_{\|}$ in Ge[4] gives good agreement with experiment. Also, her

estimated value for the spin-orbit splitting at L_3, for Ge[4] was confirmed by our detailed calculation and by the experiments of Tauc and Abraham[8] and the recent ones of Cardona and Sommers.[8] In this section, however, we shall demonstrate a case where two band approximation is no longer sufficient.

Let us assume a two band case for Si. Then, we have for the longitudinal shift

$$\delta g_{\parallel}^{Si} = \mathrm{Re}\,\frac{4}{mi}\left(\frac{1}{E_{\Delta_1}-E_{\Delta_5}}\right)^2 |\langle\Delta_1|P_y|\Delta_5^y\rangle|^2 \langle\Delta_5^y|h_x|\Delta_5^z\rangle \quad (5.8)$$

From K. and P.'s calculation only Δ_5 contributes appreciably to the electron effective mass at Δ_1. Then the value of the momentum matrix element in (5.8) can be taken from the effective mass. The s-o matrix element has been calculated for $\underset{\sim}{k}_o$ in Section IV and the energy gap can be taken from K. and P.'s band calculation. If we take $(\frac{m}{mt*})_{Si} = 5.2$,[25] $E_{\Delta_1} - E_{\Delta_5} = 4.7$ ev,[18] and $\Delta_{s-o} = .0011$ ev from (4.14), the magnitude of $\delta g_{\parallel}$ is evaluated to be $.98 \times 10^{-3}$. Next we consider the question of <u>sign</u>. From (5.8) we see that the sign of $\delta g_{\parallel}$ is determined by the sign of $\frac{1}{i}\langle\Delta_5^y|h_x|\Delta_5^z\rangle$, which can be related to the atomic core s-o matrix element by

$$\frac{1}{i}\langle\Delta_5^y|h_x|\Delta_5^z\rangle = (|b'^{\Delta_5}_{2p}|^2 - |b^{\Delta_5}_{2p}|^2)\,\frac{1}{i}\langle\chi_y|h_x|\chi_z\rangle. \quad (5.9)$$

From (4.6) and the fact that the quartic degenerate state, which corresponds to an atomic $P_{3/2}$ state, lies above the doubly degenerate one at Γ, it is readily established that the sign of $\frac{1}{i}\langle\chi_y|h_x|\chi_z\rangle$ is negative. Furthermore, from the discussion of s-o splitting and specifically from (4.11) and (4.13), we see that $|b'^{\Delta_5}_{2p}| < |b^{\Delta_5}_{2p}|$ at $\underset{\sim}{k}_o$. Then according to (5.8), $\delta g_{\parallel}^{Si}$ has a positive sign. The question of sign for $\delta g_{\parallel}^{Si}$ was first pointed out by Yafet.[26] A rough estimate for $\delta g_{\perp}^{Si}$ in the two band case gives it a negative value, the magnitude of which is one fifth of that of $\delta g_{\parallel}$.

In short, assuming a two band case for Si, the calculated values for the conduction g-tensor do not show any agreement with the experimental values[27] which not only give a negative $\delta g_{\parallel}$ but also a $\delta g_{\perp}$ larger in magnitude than $\delta g_{\parallel}$. For Ge, however, a two band calculation gives a negative $\delta g_{\parallel}$ consistent with experiment. This reversal in sign from Si to Ge is reflected in the s-o split levels for the valence band by the cross-over along Λ_3 discussed in Section IV.

Calculation of g-Tensor

From the failure of a two-band approximation, we see that the problem of g-tensor in Si is complicated. It is not possible to evaluate the shift purely from experimental parameters. For Si, we use K and P wave functions to calculate some of the matrix elements involved. First of all, because of the selection rule $\langle X_4^n | h | X_4^n \rangle = 0$, we expect that the largest contribution comes from the interband s-o matrix element $\langle \Delta_5^n | h | \Delta_5^{n'} \rangle \simeq \langle X_4^n | h | X_4^{n'} \rangle$. It is found that the most important terms in the g-shift for Si involve matrix elements of this form when one of the levels involved belongs to the 2p core state, which is far below the conduction band. The reason that such a low lying state can make important contributions to the g-shift is due to the small magnitude of the s-o splitting of the valence Δ_5 state at $\underset{\sim}{k}o$, which we have calculated in Section IV. Therefore, the gain in s-o matrix element by going to the 2p core, even after being off-set by the loss due to the energy denominator, still gives dominating contributions. In the calculation of the momentum matrix element between valence states, we follow the discussion in effective mass evaluation and use the plane wave part of the crystal wave function. In the

evaluation of the momentum matrix element involving core states, we use the Slater type analytic wave functions for the core used by Woodruff.[28] See Table II for the relative importance of different terms in calculating the Si g-tensor. The calculated results for $\delta g_{\parallel}^{Si}$ and $\delta g_{\perp}^{Si}$ are listed in Table III together with their experimental values by Wilson and Feher.[27]

After the investigation for Si, we come to ask ourselves whether a two band approximation is sufficient for Ge, especially, what is the role of the various core states involved. For this investigation, we use our own Ge crystal wave function. We do not want to consider any term in Eq. (5.3) which contains core states twice; (these are very small because of the square of a large energy denominator involved). So we have to mix one of the valence states to the conduction state by a momentum operator and then mix this valence state to one of the core states by the s-o operator in order to get any appreciable contribution to the g-tensor. Since we have seen in the previous section that there is largely 3p character in the valence states involved, we need only consider the 3p core state. Investigation along this line shows that the core contributions to both $\delta g_{\parallel}^{Ge}$ and $\delta g_{\perp}^{Ge}$ are negligible. Then, a two band approximation (L_1 and

L_3, states in Fig. 2) should be sufficient for $\delta g_{\parallel}^{Ge}$. For $\delta g_{\perp}^{Ge}$ the most important contribution comes from the first term in the appropriate formula in (5.3) when the three bands involved are L_1, L_3, and L_2^1, of Fig. 2. The contribution from other terms is very small. In particular $\Delta g_{\perp}'$ in Roth's[4] original notation amounts only to 1% of the most important term. This verifies Phillip's conjecture as mentioned in Roth's paper. Since there are very few bands involved, we can use the experimental values for the effective mass and the s-o splitting in the calculation of conduction g-tensor whenever this is applicable. The calculated values are listed in Table III.

It is to be noticed that the calculated value for $\delta g_{\perp}$ has the right magnitude but the wrong sign as compared with the experimental one by Wilson and Feher.[29] Several possible causes for this discrepancy may be mentioned. The one-electron approximation and the effective mass formalism have been tested in many ways in other experiments and in the other parameters calculated here, with good agreement between experiment and theory. The present calculation is rather insensitive to the band structure because the most important energy denominator $E_{L_1} - E_{L_3}$, is taken from experiment, and because the momentum matrix elements are close to

those of nearly free electron wave functions. Further there is no selection rule for the s-o matrix elements, which are normal. It therefore appears most likely that an error in sign has been made. A careful search has been made, but with no success.

VI. Spin-Lattice Relaxation in Si

Roth[9] has proposed a spin-lattice relaxation mechanism for donor electrons in Si, which is the whole relaxation mechanism when the magnetic field is in the (100) direction (x-direction). This mechanism, according to Roth, arises from the interaction which is responsible for the modulation of the single valley g-tensor values when the crystal is under uniaxial stress along the (111) direction. The interaction takes the following form:

$$\mathcal{H} = A\,\frac{\beta}{2}\left\{\epsilon_{yz}(\sigma_y H_z + \sigma_z H_y) + \text{cycl. perm.}\right\}, \quad (6.1)$$

where β is the Bohr magneton and ϵ_{yz} is the yz component of the strain tensor. When the Si sample is put under stress in the (111) direction, the Δ_2, state which is very close to the Δ_1 conduction band edge gets mixed into Δ_1 through the shear deformation potential component E_{yz} if the effect of crystal deform-

ation on the electronic states is treated by perturbation theory. Roth argued that in view of the small energy gap between Δ_1 and Δ_2, at the band edge (0.35 ev according to our calculation), the most important terms in the parameter A should involve Δ_2, at least twice and are equal to

$$A = \frac{4i}{3m} \frac{\langle \Delta_2, | P_x | \Delta_2, \rangle \langle \Delta_2, | E_{yz} | \Delta_1 \rangle}{E_{12}^2, E_{15}}$$

$$\left\{ \langle \Delta_1 | P_y | \Delta_5{}^y \rangle \langle \Delta_5{}^y | h_y | \Delta_2, \rangle + \langle \Delta_1 | h_y | \Delta_5{}^z \rangle \langle \Delta_5{}^z | P_y | \Delta_2, \rangle \right\} \tag{6.2}$$

We have investigated all the remaining terms in the perturbation expansion for A, paying particular attention to the core states and we have estimated that their net contribution amounts to no more than 10% of the two terms already listed in (6.2). Wilson and Feher[27] in their experiments measured the change in the conduction g value when the Si sample is put under stress along the (111) direction and hence the parameter A. On the other hand, we have calculated all the s-o and momentum matrix elements and energy gap values involved in A. Using their experimental value of A = 0.44 ± .04, we then get a value of 23 ev for $\langle \Delta_2, | E_{yz} | \Delta_1 \rangle$. This is to be compared with the intraband shear deformation

potential matrix element $E_2 = \langle \Delta_1 | E_{yy} | \Delta_1 \rangle = 7$ ev from conductivity measurements.[30]

Wilson and Feher[27] also measured the relaxation rate due to the mechanism in (6.1) and compared the experimental value with the value obtained by theoretical formula after putting A = 0.44 from the measurement of shift in g-value due to strain. They found that the theoretical relaxation rate is too slow by about a factor of 2. In other words, if we are to estimate A from the relaxation rate measurement, assuming the proposed mechanism, we would get a value for A 2 times larger than 0.44. This in turn gives a value for $\langle \Delta_2, | E_{yz} | \Delta_1 \rangle$ 2 times larger than what we estimated.

Roth[14] and Hasegawa[10] have independently proposed another mechanism for the donor spin-lattice relaxation in Si, which is caused by the change in g-value due to valley repopulation and depends primarily on $g_{\parallel} - g_{\perp}$. Wilson and Feher[27] in their experiment also measured the relaxation rate due to this mechanism. Using their measured value, Yafet[26] then estimated E_2 involved to be 20 ev. Comparison of this value with 7 ev from conductivity measurements gives us an idea about the range of error we should expect by estimating deformation potentials from spin-lattice relaxation measurements.

The author was informed that Hensel[31] was conducting an experiment to determine the change in Si electron effective mass due to strain mixing of Δ_1 and $\Delta_{2'}$, which will provide a check on our calculated results for the deformation potential matrix element.

TABLE I

CORE STATE SPIN-ORBIT SPLITTING

		Si	Ge
2p	Exp. (ev)	0.72	31
	Corr. exp. (ev)	0.60	27
	calc. (ev)	0.52	30
3p	calc. (ev)		4.0
3d	calc. (ev)		0.57

TABLE II

RELATIVE MAGNITUDE OF CONTRIBUTIONS TO g-TENSOR IN Si

	Term in (5.2) involving:			Relative magnitude with respect to first term in $\delta g_{\parallel}^{Si}$
$\delta g_{\parallel}$	$\langle\Delta_1\|p_y\|\Delta_5{}^y\rangle$,	$\langle\Delta_5{}^y\|h_x\|\Delta_5{}^z\rangle$,	$\langle\Delta_5{}^z\|p_z\|\Delta_1\rangle$	1
	$\langle\Delta_1\|p_y\|\Delta_5{}^{1y}\rangle$,	$\langle\Delta_5{}^{1y}\|h_x\|\Delta_5{}^z\rangle$,	$\langle\Delta_5{}^z\|p_z\|\Delta_1\rangle$	0.7
	$\langle\Delta_1\|p_y\|\Delta_5{}^y\rangle$,	$\langle\Delta_5{}^y\|h_x\|\Delta_5{}^{1z}\rangle$,	$\langle\Delta_5{}^{1z}\|p_z\|\Delta_1\rangle$	0.7
	$\langle\Delta_1\|p_y\|\Delta_5{}^{ty}\rangle$,	$\langle\Delta_5{}^{ty}\|h_x\|\Delta_5{}^z\rangle$,	$\langle\Delta_5{}^z\|p_z\|\Delta_1\rangle$	-2.6
	$\langle\Delta_1\|p_y\|\Delta_5{}^y\rangle$,	$\langle\Delta_5{}^y\|h_x\|\Delta_5{}^{tz}\rangle$,	$\langle\Delta_5{}^{tz}\|p_z\|\Delta_1\rangle$	-2.6
$\delta g_{\perp}$	$\langle\Delta_1\|p_z\|\Delta_5{}^z\rangle$,	$\langle\Delta_5{}^z\|p_x\|\Delta_5{}^z\rangle$,	$\langle\Delta_5{}^z\|h^y\|\Delta_1\rangle$	-0.5
	$\langle\Delta_1\|p_z\|\Delta_5{}^z\rangle$,	$\langle\Delta_5{}^z\|h_y\|\Delta_1{}^1\rangle$,	$\langle\Delta_1{}^1\|p_x\|\Delta_1\rangle$	0.3
	$\langle\Delta_1\|p_z\|\Delta_5{}^{tz}\rangle$,	$\langle\Delta_5{}^{tz}\|h_y\|\Delta_1{}^1\rangle$,	$\langle\Delta_1{}^1\|p_x\|\Delta_1\rangle$	-0.2
	$\langle\Delta_1\|p_z\|\Delta_5{}^z\rangle$,	$\langle\Delta_5{}^z\|h_y\|\Delta_1{}^t\rangle$,	$\langle\Delta_1{}^t\|p_x\|\Delta_1\rangle$	-3.1
	$\langle\Delta_1\|p_z\|\Delta_5{}^{tz}\rangle$,	$\langle\Delta_5{}^{tz}\|h_y\|\Delta_1{}^t\rangle$,	$\langle\Delta_1{}^t\|p_x\|\Delta_1\rangle$	-0.3

Note:

The first term in $\delta g_{\parallel}$ is the only one contributin in the two-band approximation.

TABLE III

G-TENSOR

		$\delta g_{\parallel}$	$\delta g_{\perp}$
	cal.	- .0027	-0.0036
Si	exp.	- .0028	-0.0040
	cal.	-1.0	+0.069
Ge	exp.	-1.13	-0.082

ACKNOWLEDGEMENTS

The author wishes to express his gratitude to Professor J. C. Phillips for suggesting the problem and many helpful comments and to Professor M. H. Cohen for interesting discussions. He is also indebted to Dr. O. C. Simpson for his hospitality at Argonne and to Dr. F. Bassani and Mr. M. Yoshimine for discussions and for allowing him to use their computer program for OPW band calculation. The atomic H-F wave function for Ge is furnished by Dr. W. W. Piper prior to publication, to whom the author extends his deep gratitude.

APPENDIX

Band Calculation for Ge

A band calculation for Ge is done by the orthogonalized plane wave method. The crystal potential is assumed to be composed of two parts, coulomb part and exchange part. For the coulomb potential a superposition of atomic charge distribution is assumed. The atomic H-F wave function for Ge is furnished by Piper. For the exchange potential we adopt Slater's approximation

$$V^{ex}(\underset{\sim}{r}) = -6\left[\frac{3}{8\pi}\,\rho(\underset{\sim}{r})\right]^{1/3} \qquad (A.1)$$

lumping both core and valence charge densities together. The valence wave function is orthogonalized to atomic core wave function and the orthogonalization coefficients A_t are listed in Table IV. Note that the orthogonalization coefficients B_t in all the formulae related to the s-o splitting in this paper differ from the listed A_t by a factor of $\sqrt{2}$ ($B_t = \sqrt{2}\,A_t$). This is

because there are two atoms per unit cell for diamond structure and we have included a $1/\sqrt{2}$ factor in the core function $\phi^{\alpha}_{k,t}$ in (3.2) to have it properly normalized. By taking $V_{000} = -2.58$ ry according to F. Herman (Physica 20, 801, 1954), we have obtained the energy eigen-values (Table V) and eigen-vectors for states at Γ and L. The energy bands thus obtained agree qualitatively with a similar calculation by Herman, except that our calculation gives a Γ_{15} state lower than $\Gamma_{2'}$ state in energy, in contradiction with both Herman's calculation and experiment. However, an adjustment of the value for V_{000} can bring down $\Gamma_{2'}$ relative to Γ_{15} state and produce a value for the conduction-valence gap at Γ and L in agreement with experiment. For the most crucial gap value $E_{L_1} - E_{L_3}$, in our g-tensor calculation we have used experimental value. Moreover, the calculated crystal band s-o splitting value depends primarily on the magnitude of the orthogonalization coefficients, the accuracy of which depends on that of H-F atomic core wave function. The plane wave coefficients are not even sensitive to band calculations for different substances of the same crystal structure. For example, comparing the Si result by K and P and the Ge result by us, we often find agreement to at least the first figure

between the corresponding plane wave coefficients for some of the important states. Therefore, no attempt has been made to recalculate the eigen-values and eigen-vectors with different choices of V_{000}. The calculated values for the plane wave coefficients for various states of Ge are contained in Table VI.

TABLE IV

ORTHOGONALIZATION COEFFICIENTS FOR Ge

$\lvert \underset{\sim}{k}+\underset{\sim}{K} \rvert^2$	A_{1s}	A_{2s}	A_{3s}	$-iA_{2p}$	$-iA_{3p}$	A_{3d}
0	.00469	-.03287	.15285	.00000	.00000	.00000
3	.00468	-.03193	.12669	.00560	-.08660	.15462
4	.00468	-.03167	.11920	.00641	-.09390	.20933
8	.00467	-.03066	.09385	.00878	-.10505	.28967
11	.00466	-.02994	.07872	.01006	-.10479	.29512
12	.00467	-.02970	.07427	.01043	-.10393	.29310
16	.00464	-.02879	.05892	.01169	-.09848	.27682
19	.00463	-.02813	.04952	.01246	-.09330	.26109

TABLE V

ENERGY EIGEN-VALUES (IN Ry. FOR Ge)

Γ_1	$L_{2'}$	L_1^1	$L_{3'}$	$\Gamma_{25'}$	L_1	Γ_{15}	$\Gamma_{2'}$	L_3	$L_{2'}^1$
-1.924	-1.704	-1.523	-1.172	-1.036	-0.824	-0.792	-0.765	-0.730	-0.478

TABLE V

ENERGY EIGEN-VALUES (IN Ry. PER De)

TABLE VI

PLANE WAVE COEFFICIENTS FOR GE

$(\underset{\sim}{k}+\underset{\sim}{K})$	Γ_1	$\Gamma_{25'}$	$\Gamma_{2'}$	Γ_{15}
(000)	0.977			
(111)	-0.361	.796	.974	.990
(200)		.669	.536	
(220)	0.007	-.006		.316
$(311)_1$	0.061	-.148	.099	.113
$(311)_2$		-.073		.110
(222)	0.018	-.094	.076	.026
(400)	0.038			.020
$(331)_1$	-0.037	-.006		
$(331)_2$			.068	-.014

	$L_{2'}$	L_1^1	$L_{3'}$	L_1	L_3	L_2^1
(1/2 1/2 1/2)	1.013	.946		.190		-.178
(3/2 1/2 1/2)	- .217	.346	1.002	-1.054	.820	-.945
(3/2 3/2 1/2)	.160	.249	- .149	.286	-.503	-.085
(5/2 1/2 1/2)	- .033	.025	.188	.089	.110	-.263
(3/2 3/2 3/2)	.123	-.127		- .025		-.119
$(5/2\ 3/2\ 1/2)_1$	- .097	.047	.085	.022	-.254	.049
$(5/2\ 3/2\ 1/2)_2$			.134		-.405	
(5/2 3/2 3/2)	- .058	-.034	.128	.058	-.106	-.074
(5/2 5/2 1/2)	- .042	-.054	- .004	- .042	.043	-.009
(7/2 1/2 1/2)	.070	.034		- .030		.041

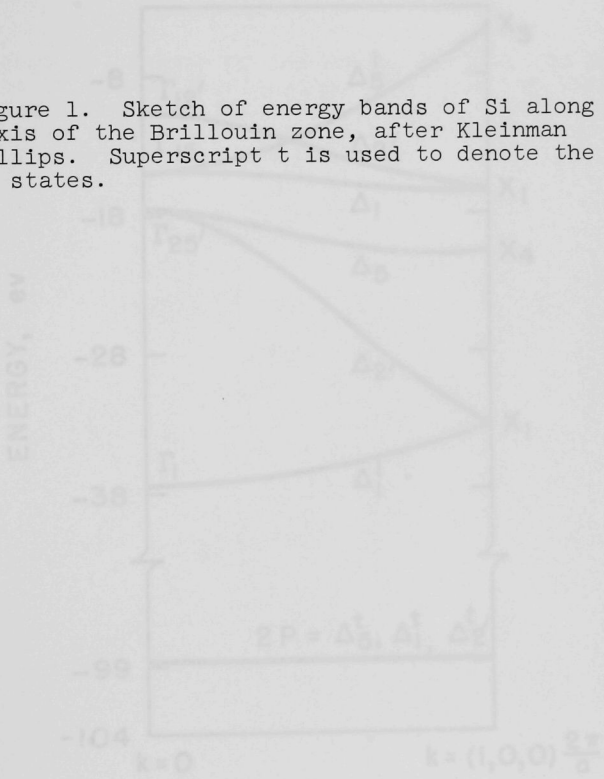

Figure 1. Sketch of energy bands of Si along [100] axis of the Brillouin zone, after Kleinman and Phillips. Superscript t is used to denote the 2p core states.

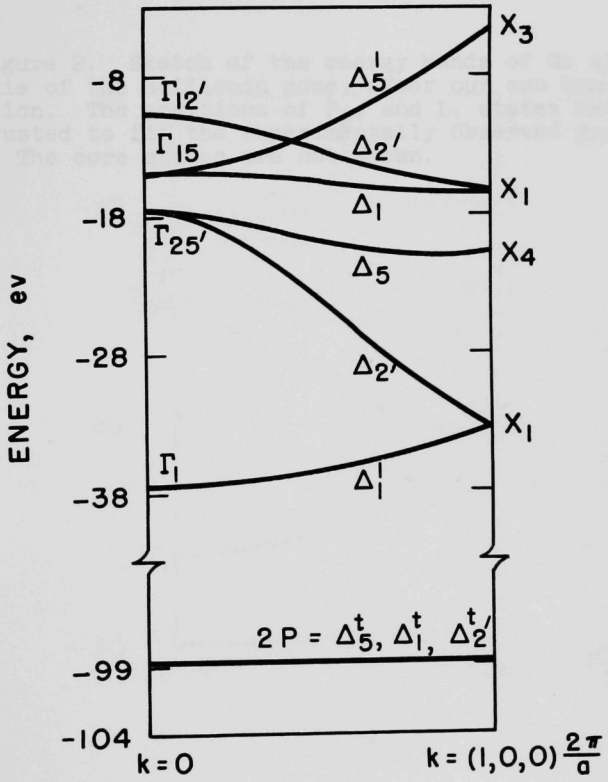
ENERGY, ev
-8
-18
-28
-38
-99
-104
$\Gamma_{12'}$
Γ_{15}
$\Gamma_{25'}$
Γ_1
Δ_5^1
$\Delta_{2'}$
Δ_1
Δ_5
$\Delta_{2'}$
Δ_1^1
X_3
X_1
X_4
X_1
$2P = \Delta_5^t, \Delta_1^t, \Delta_{2'}^t$
k = 0
k = (1,0,0) $\frac{2\pi}{a}$

ENERGY, eV
-8
-18
-28
-38
-104
k = 0
k = (1,0,0) 2π/a
X3
X1
X4
X1
L1
L2S1
L1S1
Δ5
Δ1
Δ1
Δ5
Δ5
Δ1
Δ2'
Δ1
Δ2
S.P. = Δ5, Δ1, Δ1, Δ2', Δ1

Figure 2. Sketch of the energy bands of Ge along [111] axis of the Brillouin zone, after our own band calculation. The positions of $\Gamma_{2'}$ and L_1 states have been adjusted to fit the experimentally observed gap values. The core states are not shown.

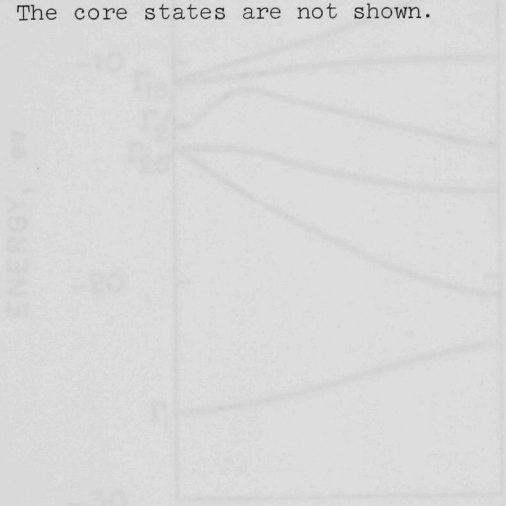

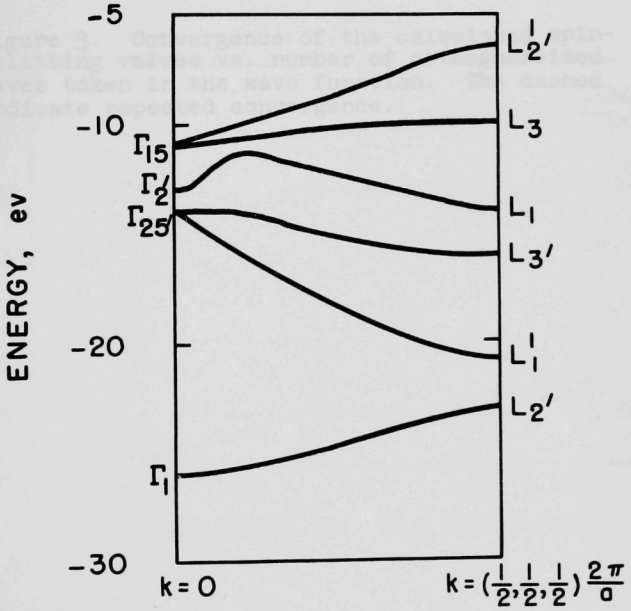
-5
-10
-20
-30
ENERGY, ev
Γ_{15}
Γ_2'
$\Gamma_{25'}$
Γ_1
$L_2^1{}'$
L_3
L_1
$L_{3'}$
L_1^1
$L_{2'}$
k = 0
$k = (\frac{1}{2}, \frac{1}{2}, \frac{1}{2}) \frac{2\pi}{a}$

-5
-10
-20
-30
ENERGY, eV
k = O
Γ1
Γ25'
Γ12
Γ15
Γ2
Γ15
Γ25
Γ1
Γ25'
Γ12

Figure 3. Convergence of the calculated spin-orbit splitting values vs. number of orthogonalized plane waves taken in the wave function. The dashed lines indicate expected convergence.

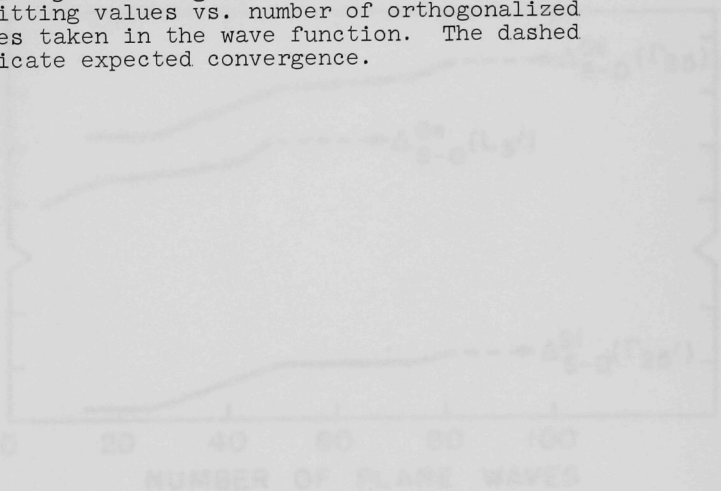

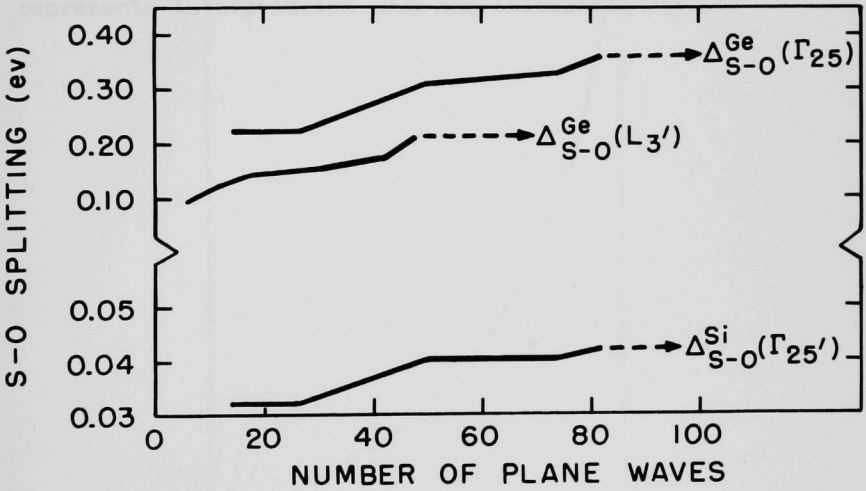
S-O SPLITTING (ev)
0.40
0.30
0.20
0.10
0.05
0.04
0.03
0
20
40
60
80
100
NUMBER OF PLANE WAVES
$\Delta^{Ge}_{S-O}(\Gamma_{25})$
$\Delta^{Ge}_{S-O}(L_{3'})$
$\Delta^{Si}_{S-O}(\Gamma_{25'})$

$\Delta^{Ge}_{S-O}(\Gamma_{28})$
$\Delta^{Ge}_{S-O}(L_3)$
$\Delta^{Si}_{S-O}(\Gamma_{28'})$
0.40
0.30
0.20
0.10
0.05
0.04
0.03
0
20
40
60
80
100
NUMBER OF PLANE WAVES
S-O SPLITTING (eV)

Figure 4. Sketch of the spin-orbit splitting of the Δ_5 valence band of Si. The dashed curve represents interpolation from the calculated results.

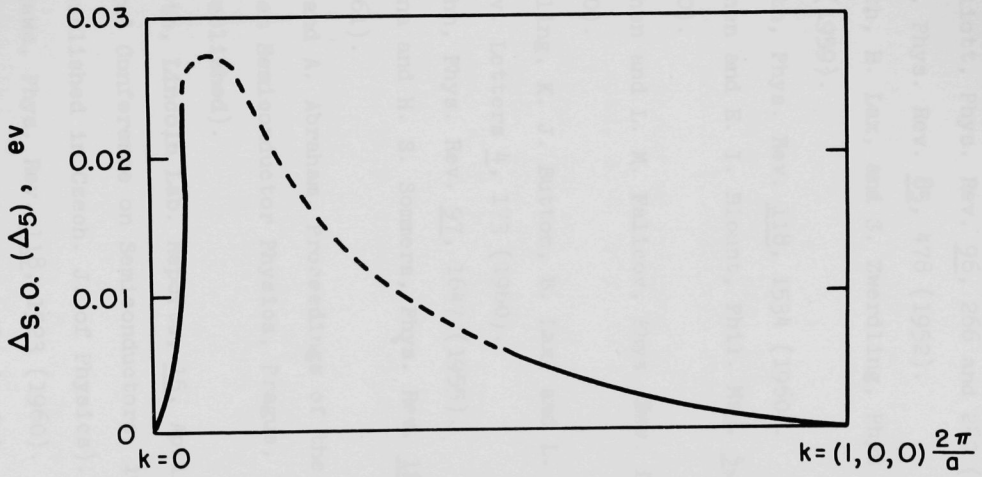
0.03
0.02
0.01
0
$\Delta_{S.O.}(\Delta_5)$, ev
k = 0
k = (1, 0, 0) $\frac{2\pi}{a}$

K=0
0
0.01
0.02
0.03

REFERENCES

1. R. J. Elliott, Phys. Rev. 96, 266 and 280 (1954).
2. Y. Yafet, Phys. Rev. 85, 478 (1952).
3. L. M. Roth, B. Lax, and S. Zwerdling, Phys. Rev. 114, 90 (1959).
4. L. M. Roth, Phys. Rev. 118, 1534 (1960).
5. M. H. Cohen and E. I. Blount, Phil. Mag. 5, 115 (1960).
6. M. H. Cohen and L. M. Falicov, Phys. Rev. Letters 5, 544 (1960).
7. S. Zwerdling, K. J. Button, B. Lax, and L. M. Roth, Phys. Rev. Letters 4, 173 (1960).
8. A. H. Kahn, Phys. Rev. 97, 1647 (1955).
   M. Cardona and H. S. Sommers, Phys. Rev. 122, 1382 (1961).
   J. Tauc and A. Abraham, Proceedings of the Conference on Semiconductor Physics, Prague, 1960 (to be published).
9. L. M. Roth, Lincoln Lab. Reports, 15, April 1960, and Prague Conference on Semiconductors, 1960 (to be published in Czech. J. of Physics).
10. H. Hasegawa, Phys. Rev. 118, 1523 (1960).
11. L. Liu, Phys. Rev. Letters 6, 683 (1961).
12. L. L. Foldy and S. A. Wouthysen, Phys. Rev. 78, 29 (1950).

13. W. W. Piper, to be published.

14. C. E. Moore, Atomic Energy Levels (National Bureau of Standards).

15. J. C. Phillips, Phys. Rev. 112, 685 (1958).

16. D. H. Tomboulian and W. M. Cady, Phys. Rev. 59, 422 (1944).

17. F. Tyren, Ark. Math. Astr. Fys. A25, Nr. 32 (1937).

18. L. Kleinman and J. C. Phillips, Phys. Rev. 118, 1153 (1960) Hereafter referred to as K and P.

19. F. Englert, Acad. R. d. Belg. Bull 43, 273 (1957). ψ_z and ψ_y in Eqs. (5) and (6) of this paper should be interchanged. Also Eqs. (27)-(29) are in error.

20. G. Dresselhaus, A. F. Kip and C. Kittel, Phys. Rev. 98, 368 (1955).

21. G. Dresselhaus, Ph.D. Thesis, University of California, 1955 (unpublished).

22. B. Lax, Rev. Modern Phys. 30, 122 (1958).

23. H. R. Philipp and E. A. Taft, Phys. Rev. 113, 1002 (1959).

24. R. N. Dexter, H. J. Zeiger, and B. Lax, Phys. Rev. 104, 637 (1956).

25. C. J. Rauch, J. J. Stickler, H. J. Zeiger and G. S. Heller, Phys. Rev. Letters 4, 64 (1960).

26. Y. Yafet, Private Communication.

27. D. K. Wilson and G. Feher, (to be published).

28. T. O. Woodruff, Phys. Rev. 103, 1159 (1956).

29. D. K. Wilson and G. Feher, Bull. Am. Phys. Soc. II5, 60 (1960).

30. R. W. Keyes, Solid State Physics, Vol. II., Acad Press (1960).

31. J. C. Hensel, Private Communication.